



Evaluation of floc settling velocity models through image analysis for ballasted flocculation

Muhammad Qasim¹, Seongjun Park¹, Jinsil Lee, Jong-Oh Kim*

Department of Civil and Environmental Engineering, Hanyang University, 222 Wangsimni-ro, Seongdong-gu, Seoul 04763, Korea, Tel. +82-2-2220-0325; Fax. +82-2-2220-1945; email: jk120@hanyang.ac.kr (J.-O. Kim), Tel. +82-2-2220-4703; emails: engrqasim00@hanyang.ac.kr (M. Qasim), Jayenv93@hanyang.ac.kr (S. Park), trutha2@naver.com (J. Lee)

Received 15 March 2018; Accepted 6 August 2018

ABSTRACT

The outstanding performance of ballasted flocculation (BF) can be attributed to the enhanced velocity of settling flocs, which is significantly increased by the attachment of ballast particles. It is important to determine the mechanism by which the settling velocity of an individual floc changes with ballast size and density under BF. Many researchers have developed models to predict floc settling velocity, which is correlated with the size and density of flocs, but these existing models underestimate the floc settling velocity because model parameters are not obtained from flocs of BF. Therefore, the purpose of this study is to improve the accuracy of model prediction of floc settling velocity by modifying existing regression models based on experimental observations. For this purpose, an image analysis method was used to determine the settling velocity and size of individual flocs generated through laboratory BF experiments, and then floc density was calculated using Stokes' law with flow condition-based drag coefficient. These velocity and density values were used to compare and modify the velocity models. The predictions of modified models and the experimental observations were then tested through analysis of variance and Pearson's correlation. The modified density model of Lau and Krishnappan was found to be the most appropriate for predicting individual floc density, but velocity models as linear or power function of floc size were inappropriate for predicting the settling velocity of ballasted flocs. Various statistical tests revealed that the modified velocity model is effective. In addition, the model predictions were found to be in agreement with 75% of experimental velocity observations, whereas other velocity models showed only 30% agreement. Thus, we propose the combination of the Stokes' velocity model with the modified density model of Lau and Krishnappan as the most suitable approach for predicting settling velocity.

Keywords: Ballasted flocculation; Floc density; Settling velocity modelling; Magnetic ballast; Image analysis

1. Introduction

Recently, ballasted flocculation (BF) has received significant attention as an alternative for treating influent turbidity, which is being aggravated by global climate change. Research has revealed the outstanding performance of BF in turbidity treatment of municipal and industrial wastewater, and the application field of BF has been extended to the treatment of

drinking and surface waters [1]. In BF, the specific gravity of flocs is increased by the attachment of high-density ballasts that significantly enhances the settling velocity of flocs [2]. Floc formation with ballasts is a complicated process because its simultaneous and dynamic mechanisms include aggregation, fragmentation, repacking, remineralization, deposition, and eventually subsequent resuspension [3]. The causes and effects from these mechanisms can converge to settling velocity. Therefore, it is important to predict and measure

¹ Joint first authors

* Corresponding author.

the settling velocity of individual flocs theoretically and experimentally [4].

Numerous attempts were made to model floc settling velocity as a function of floc shape, size, and density. Among these, floc density is known to be an important factor driving floc settling [5], and its value is varied from discrete particle settling to flocculent particle settling [2]. Few studies indicated that floc density can be directly measured and floc settling velocity can be determined accordingly, while others indicated that individual floc density is very difficult to determine directly [6]. The most common approach is to determine the density from experimentally determined floc settling velocity by applying appropriate models that correlate floc density and settling velocity [7,8]. In determining the settling velocity and density, the floc size should be always obtained concurrently, irrespective of the models used [4]. Photographic methods through image analysis are the most reliable for determining floc size as well as floc settling velocity [5]. When floc size and settling velocity are experimentally determined, Stokes' law can be applied to determine floc density [8].

Previous studies developed models based on Stokes' law to reflect the effect of floc shape, size, permeability, porosity, and fractal dimensions on the physical characteristics of generated flocs [9–11]. Floc density models are derived on the basis of physical and mathematical relationships, which account for the density of parent particles in suspension, using the concept of mass balance and fractal dimensions [12]. Some researchers reported floc density as a function of projected floc area in the form of regression equations [13–15]. Although the ballasted floc settling phenomenon is difficult to directly observe, it can be reflected through model.

In this study, we developed a suitable model to investigate ballasted floc settling velocity. The main purpose is to evaluate and modify existing floc density and settling velocity models to reflect BF. In comparison with the conventional flocs, ballasted flocs have different physical characteristics (especially much higher floc density induced because of ballast) and they show much higher settling velocity. Therefore, jar tests were conducted to obtain the ballasted floc using four different types and varied doses of ballasts, and the correlation between floc size and density was confirmed through image analysis. Based on Stokes' law, floc density from experimental velocity observations was compared with existing models. Then, the existing models were modified using regression analysis based on experimentally determined floc size, settling velocity, and effective floc density to improve their applicability for ballasted flocs. The modified model predictions were plotted graphically along with experimental values to establish the significance of the modified models. Analysis of variance (ANOVA) was applied to observe the differences in agreement among experimental values and model predictions.

2. Materials and methods

2.1. Evaluation of existing models

Floc density models developed by Tambo and Watanabe [8], Hawley [6], McCave [13], and Lau and Krishnappan [14] were investigated in this study. These models were developed

on the basis of experimental observations of flocs formed naturally in estuarine systems or conventional flocculation. The applicability of these existing density models (Table 1) was evaluated by comparing model predictions with a designated floc density, and the results revealed that the density models completely underestimated the determined floc density for ballasted flocs. The reason of the underestimation is that the density models were developed to predict flocs in estuarine systems or conventional flocculation systems where floc size increases slowly and floc density is low. In BF, charged particles using coagulants [16] and high-density flocs with ballast particles are combined for faster settling. The existing density models presented in Table 1 can be used for determining ballasted floc density if modified according to experimental observations of ballasted flocs.

Li and Ganczarczyk [4], Adachi and Tanaka [17], and Wu and Lee [15] developed floc settling velocity models using floc size measured from jar tests replicating conventional flocculation processes. These existing settling velocity models (Table 1) were graphically simulated with experimental velocity based on image analysis observations. In preliminary comparisons, no agreement was found among model predictions and BF experimental observations because the effect of ballasts was not incorporated in these existing models. The obvious limitation of these simple models is that the models do not account for the effect of ballast as floc size is only variable in these models.

Preliminary experiments also revealed that the relationship between floc size from the projected area of image analysis and settling velocity was insufficient to represent many other characteristics of flocs that act as driving factor controlling settling velocity. As floc density can be better predicted as a function of floc size through empirical relationships, the Stokes' floc settling velocity model can be extended based on the modified density models.

2.2. Floc formation process

In this study, high-turbidity (190 NTU) raw water was synthesized using 200 mg kaolin/L with tap water. Poly aluminum chloride (PAC) (Al_2O_3 , 10%) as coagulant and four types of magnetic ballast particles of 25 μm (negative surface charge), 33 μm (negative surface charge), 33 μm (positive surface charge), and 64 μm (negative surface charge) (Bioneer Co., Daejeon, Korea) as ballasted coagulants were used to monitor the effect of ballasts on agglomeration characteristics and floc settling velocities. Zeta potential analysis was performed to confirm the surface charge of ballast particles, and ballast size was confirmed by scanning electron microscope (SEM) images. The density, zeta potential, and chemical formula of ballast particles and SEM images of ballast particles are provided in Table S1 and Fig. S1, respectively, in supplementary materials. For generating high-density flocs, the water samples were agitated in a 1 L 6-array jar tester (Fig. S2 in supplementary materials) by rapid (G-161/s) and slow mixing (G-65/s) to replicate coagulation and flocculation processes [18,19]. The PAC dose of 30 mg/L was used, and the ballasted coagulant doses were varied to 500, 750, 1,000, 1,250, 1,500, 2,000, 2,500, 3,000, and 5,000 mg/L for four types of ballasts. The pH of the samples was adjusted to 8 using 1M sodium hydroxide solution [20]. The initial temperature of the samples was maintained at 20°C [21].

Table 1
Existing and modified floc density and settling velocity models

Sr. No.	Existing model	Particle type	Units	Reference	Modified model
Floc density models					
1	$\rho_f - \rho_w = \frac{0.0013}{\left(\frac{D_f}{1}\right)^{0.9}}$ *	Al-kaolinite clay flocs	$\mu\text{m, g/cm}^3$	[8]	$\rho_f - \rho_w = \frac{166.21}{\left(\frac{D_f}{1}\right)^{1.2}}$
2	$\rho_f - \rho_w = \rho_s - \rho_w \left(\frac{D_f}{d_s}\right)^{-0.9}$	Lacustrine aggregates	cm, g/cm^3	[6]	$\rho_f - \rho_w = (\rho_s - \rho_w) \left(\frac{D_f}{d_s}\right)^{-0.31}$
3	$\rho_f - \rho_w = 1 \quad D_f \leq 1\mu\text{m}$ $\rho_f - \rho_w = D_f^{0.42} \quad 1 \leq D_f \leq 50\mu\text{m}$ $\rho_f - \rho_w = D_f^{-1.3} \quad 50 \leq D_f \leq 1200\mu\text{m}$ $\rho_f - \rho_w = 0.003 \quad D_f \geq 1200\mu\text{m}$	Suspended particles in seawater	$\mu\text{m, g/cm}^3$	McCave (1984)	$\rho_f - \rho_w = D_f^{-0.29}$
4	$\rho_f - \rho_w = \rho_s \exp(-0.02D_f^{1.85})$	–	cm, g/cm^3	Lau and [14]	$\rho_f - \rho_w = (\rho_s - \rho_w) \exp(-0.05D_f^{0.61})$ **
Settling velocity models					
5	$V_f = 0.35 + 1.77D_f$	Activated sludge	mm, mm/s	Li and Ganczarczyk (1979)	$V_f = 6.4 + 5.6D_f$
6	$V_f = 0.969D_f^{1.150}$	Al-kaoline floc	mm, mm/s	[17]	$V_f = 10.77D_f^{0.23}$
7	$V_f = 1.17D_f^{0.99}$	Activated sludge	m, m/s	[15]	$V_f = 0.053D_f^{0.23}$

*For a dimension coincidence, dimensionless floc diameter was used in the equation because the fractal concept did not exist at the time the equation was developed.

**Modified model-4 is computed using floc size in micrometers and effective parent particle density is induced in modified model instead of parent particle density in reported model.

The jar test experimental conditions are shown in Table S2 of supplementary materials.

2.3. Determination of floc characteristics

An image analysis technique was adopted to experimentally observe the relationship between the size and settling velocity of ballasted flocs. Experimental velocity observations were then used to determine effective floc density based on Stokes' law.

The flocs formed in the jar test were subjected to image analysis [22,23], in which a vertical column image analyzer with a transparent floc settling column, charge-coupled device (CCD) camera (Mako G-507C PoE Model and Zoom lens 0.70X–4.50X, 23.7 frames/s), light emitting diode (LED) light (Figs. S3 and S4 in supplementary material) with StreamPix software program (STP-6-S-STD), and a public domain Image-J program were used. The flocs were passed through the transparent vertical column of image analyzer filled with water while CCD camera and LED light were horizontally aligned covering a specific known frame area of the vertical column to record vertical settling movement of the flocs [24]. The vertical movement with respect to time in a known column length covered by the CCD camera was

recorded using StreamPix software. The settling velocity of the flocs was determined by the vertical movement of the flocs in a known column length per time. The frames in video files for selected flocs were converted to the image format. Despeckle noise tool of Image-J program was applied to improve the floc visibility by removing the background noise and blurred flocs in the image. Threshold tool of Image-J program was used to precisely reveal the boundaries of flocs in the image. Size of flocs was determined by precisely marking the outer boundaries of flocs using the freehand marking tool of Image-J program to calculate the number of pixels covered by one floc. The actual floc projected area could be determined by multiplying the determined number of pixels with the unit pixel area and magnification. The applied tools of Image-J program and a flow chart of image analysis process are illustrated in Figs. S5 and S6 in supplementary materials.

Floc density was determined using floc settling velocity through Stokes' law which can be used for determining floc density based on floc velocity observations in the form of Eq. (1) [25,26]. The flocs were assumed to be spherical in shape, and equivalent size sphere diameter determined by Eq. (4) was applied in Eq. (1). It is very important to know the flow condition to determine the drag force applied at passing flocs by fluids inside the column for accurately calculating

Eq. (1). For this purpose, the Reynolds number for flocs was determined using Eq. (3) based on floc size and floc settling velocity (obtained through the image analysis). Eq. (3) shows that flocs follow transitional flow conditions, and thus, Eq. (2) for transitional flow conditions was used to determine drag force coefficient, which was substituted in Eq. (1) to determine effective floc density.

$$V_f^2 = \frac{4g(\rho_f - \rho_w)D_f}{3C_d \rho_w} \tag{1}$$

$$C_d = \frac{24}{Re} + \frac{3}{Re^{0.5}} + 0.34 \tag{2}$$

$$Re = \frac{\rho_w V_f D_f}{\mu} \tag{3}$$

$$D_f^2 = \frac{4A_p}{\pi} \tag{4}$$

2.4. Modification of existing models

The models were modified using the user-defined model fitting tool in the analysis wizard of OriginPro 2016 software. The model equations were input in OriginPro 2016 after replacing constants into notations as described in Table S3 in supplementary materials. The floc size was defined as independent variable X and deterministic floc density and floc settling velocity as dependent variables Y. The experimental

floc size and their corresponding determined density and settling velocity values were used in the program as input data for regression analysis to modify the models. The notations in input equations were defined as variables in the program. The values for constants in model equations were then recomputed at successful model fitting status at experimental floc size, settling velocity, and determined floc density values using the same units as mentioned in Table 1 corresponding to equations. The values for constants computed by the program were then replaced by notations to obtain modified model equations. The modified models with recomputed constant values are provided in Table 1. Fig. 1 shows a schematic diagram of the model modification process using ballasted floc generation and observation experiments. The process of model fitting and recomputing of variables for equations in OriginPro 2016 is presented in Fig. S7 in supplementary materials.

2.5. Statistical testing of modified models

ANOVA, which is used to determine whether there are any statistically significant differences between the means of independent groups, was applied to compare the model-predicted data sets with experimental data sets or determined data sets based on experimental observations to determine variations in model predictions. For this purpose, the one-way ANOVA tool of OriginPro 2016 was used. The test was conducted at a significance level of 0.05, which is generally used in ANOVA by maintaining a 5% margin of error at a confidence level of 95%. The data sets were provided in the form of raw data instead of indexed, and the number of levels were selected according to the number of

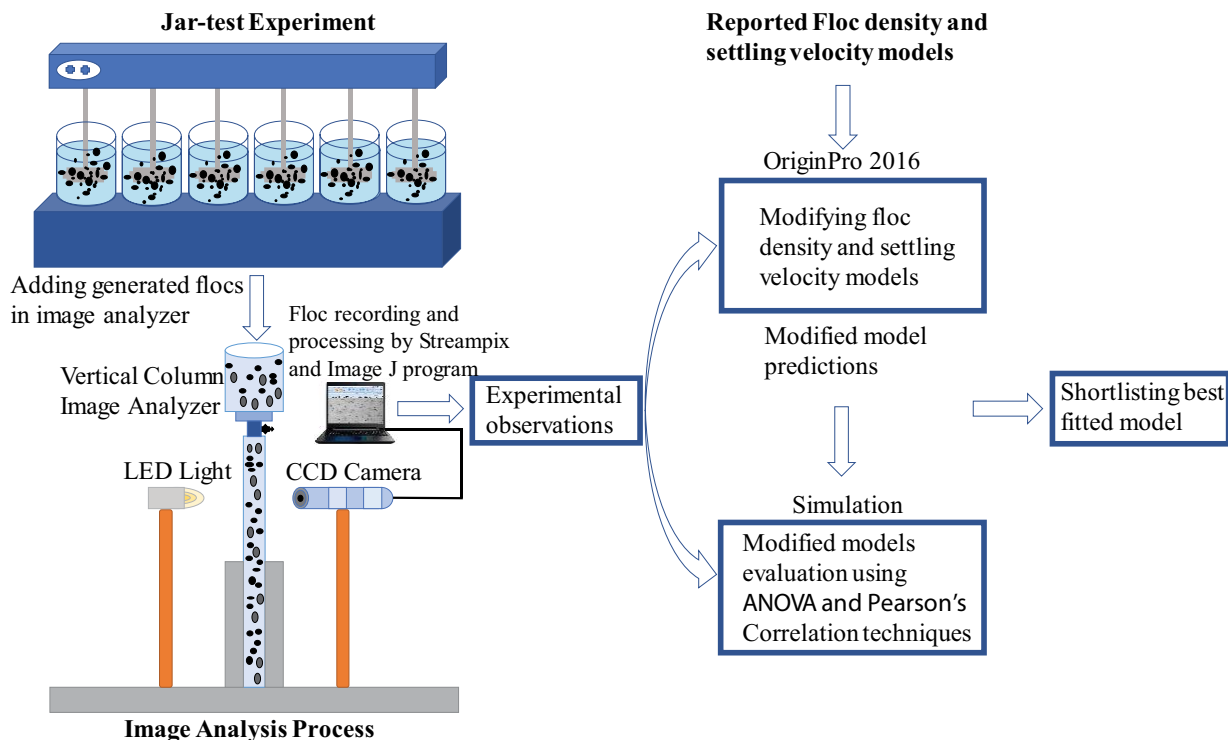


Fig. 1. Schematic diagram of BF experiment and model modification process.

data sets under comparison. Tukey's range test which is an inferential statistic used to access the equality of variance was also applied in conjunction with ANOVA, in which the set of all pair-wise comparisons was simultaneously applied and any difference between two means that is greater than the expected standard error could be identified. Tukey's test works under assumptions that observations are independent among and within groups and homogeneity of variance exists. In this study, homogeneity of variance was assured using Levene's test in conjunction with ANOVA and Tukey's test. p -value is an indicator of Levene's test, which should be less than the benchmarked significance level (0.05) for the test to approve the hypothesis of equality of variance. Box charts were obtained to evaluate the data set prediction ranges compared with experimental observations.

In ANOVA, the important indicators are F -value, root mean square of error (RMSE), coefficient of variation, and R^2 value. The F -value indicates the variation between sample means by the variation within samples; under the null hypothesis that data means are equal at all stages, it should be equal to 1. As it approaches to 1, the predicted data set will also be closer to the experimental value. RMSE is a measure of differences between model predictions and experimental observations. It indicates the degree to which experimental observations are spread out and their distance from the model line. It should be equal to zero if the model completely satisfies experimental observations. Lower RMSE indicates less variations of observed values from the model. Coefficient of variation is a ratio of standard deviation to the mean value. It shows the extent of variability in relation to the mean of the data set, and its lower value is favorable in the test. The R^2 value shows the correlation among data sets from the range of zero to one with one showing 100% correlation. It is usually ignored in ANOVA, but in the case of model comparison with experimental observations, it becomes an extremely important factor indicating the model's ability to predict experimental observations. R^2 values close to one show that the model can more accurately predict experimental values.

Pearson's correlation was also applied to measure the linear correlation between two sets of independent variables.

Its value lies between +1 and -1, where 1 is total positive linear correlation, 0 is no linear correlation, and -1 is total negative linear correlation. Its significance indicates the significant statistical relationship between two independent data sets. In this study, the Pearson's correlation tool of IBM SPSS Statistics 24 program was used to compare the model-predicted data sets with experimental or experiment-based data sets. The test was performed at a significance of 0.01 and a confidence level of 99% maintaining a 1% margin of error. The Pearson's coefficient obtained is an indicator of a linear relationship between model predictions and experimental observations. The relationship is significant only if the obtained test significance value is less than the benchmarked significance level of test.

3. Results and discussion

3.1. Determination of floc characteristics

The vertical movement of flocs along the known column height was recorded against time for each jar test condition using SreamPix in the image analysis process. At least 40 flocs from each jar test condition were analyzed to ensure adequate representation of floc distribution [24,27]. The distance covered by individual flocs was divided by the respective time consumed to determine the settling velocity of the flocs. The sizes of respective flocs were determined using Image-J. To determine the effective density of flocs using Eq. 1, the drag coefficient must be computed, which is directly related to the flow condition of floc transition in fluids. Therefore, drag coefficient was determined as a function of Reynolds number. Most of the previous studies indicated ($Re \leq 1$) vertical settling of flocs in water and used the laminar flow equation to determine the drag coefficient [9,17]. In this study, Reynolds number was determined for ballasted flocs using Eq. (2) [2], and it was observed that ballasted flocs follow the transitional flow condition ($Re > 1$), as displayed in Fig. 2(a). Reynolds number for ballasted flocs varied from 0.2 to 12, and the major proportion of flocs showed Reynolds number between 2 and 4. Furthermore, a peak of normal distribution

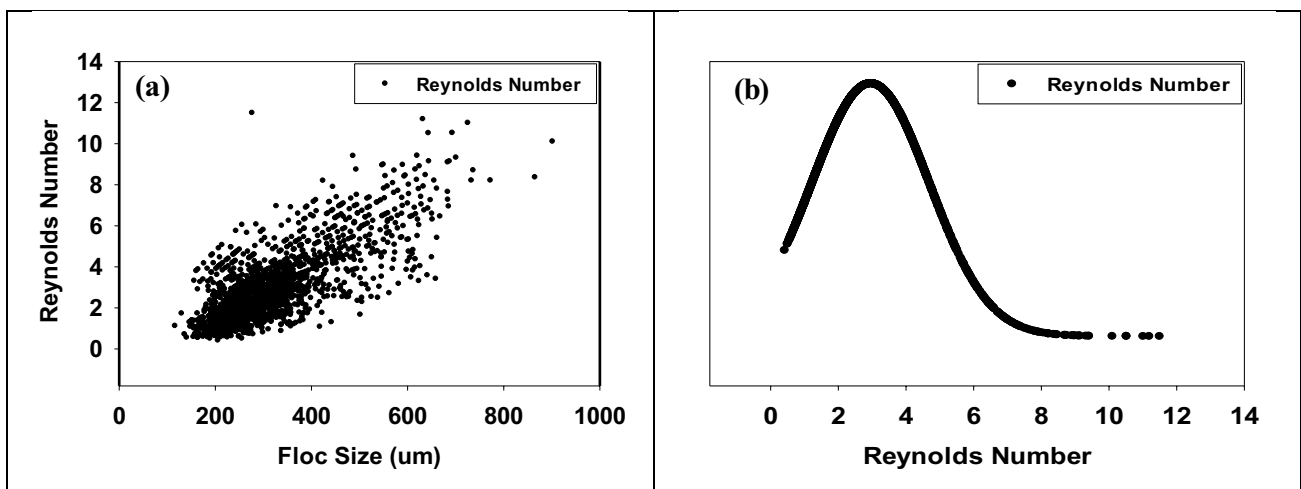


Fig. 2. Reynolds number determination for ballasted flocs: (a) Reynolds number and (b) normal distribution of Reynolds number for ballasted flocs.

curve was found at a Reynolds number of 2.98, as shown in Fig. 2(b). From these results, it was concluded that Eq. (2), which depicts drag coefficient as a function of Reynolds number under transitional flow conditions, was more suitable for determining the coefficient for drag force acting on ballasted flocs, as presented in Table S4 in supplementary materials.

The determined Reynolds number values were used to compute the drag coefficient [Eq. (2)]. The flocs were assumed to be spherical in shape and equivalent size, and the sphere diameters were obtained using Eq. (4). The computed drag coefficient values and equivalent size sphere diameters were applied in Eq. (1) to determine the effective floc density against experimental velocity observations. The experimental settling velocity and determined effective floc density were plotted against floc size to observe their variation against floc size. Floc settling velocity was also plotted against effective floc density to observe the relationship among these two properties. It was observed from the plots that floc size does not appear to have a clear relationship with floc settling velocity for ballasted flocs, whereas in conventional coagulation processes and flocculation in natural waters, flocs have been found to have strong direct proportionality with settling velocity [25]. However, the floc size was found to be in partial inverse proportionality with floc density which was in agreement to Lee et al. [28] and Gregory [29]. Floc density was partially in direct proportionality with floc settling velocity, as shown in Figs. 3(a)–(c).

3.2. Modification of existing models

The existing models shown in Table 1 were modified based on experimentally determined floc size, settling velocity, and determined floc density data sets obtained through image analysis [30]. The models were input as equations with constants and variables defined in the program. Experimental floc size values were input as independent variables and experimental settling velocity and determined floc density values were input as dependent variables. The constant values in models were recomputed by fitting the model curve of experimental values by applying the model fitting tool. The program describes the status of success or failure for model fitting of defined equations, and constant values obtained with successful fitting status were applied

in model equations to obtain the modified models. The modified models obtained by curve fitting with experimental observations are shown in Table 1.

3.3. Evaluation of modified floc density models

The determined effective floc density based on experimental velocity observations was simulated using existing density models, and the results show that the modified models predicted the density values more closely but the existing models underestimate the density values, as shown in Fig. 4(a). Among existing models, the model by Lau and Krishnappan completely failed to predict effective density for observed floc sizes because of its limitation that prediction of effective floc density is limited to flocs less than 300 μm; however, the observations were still underestimated even within this size range. Furthermore, flocs generated through BF are mostly above this size and have high density because of ballast particles induced in the flocs. The modified model predictions were graphically plotted against determined floc density, and they were found to be in complete agreement with experimental observations as shown in Fig. 4(b). To observe the correlation among determined density values and modified model predictions more closely, the Weibull distribution was applied, and the curve of determined density values was compared with the curves of the modified models. The predictive curves for modified models of Tambo and Watanabe and Lau and Krishnappan were found to be more closely correlated to the determined density curve, as shown in Fig. 4(c). It can thus be concluded that the above-mentioned models could predict the effective floc density more closely compared with others.

The percentile-percentile (*P-P*) plots of modified density models were developed, which are shown in Figs. 5(a)–(d). The straight line in the probability plot represents the model normality. A departure of determined density residuals from the straight line refers to a divergence from the model. Remarkable divergence was observed for most models as shown in Figs. 5(a)–(c), but the density residuals followed a linear trend for modified model of Lau and Krishnappan, as shown in Fig. 5(d). The model *P-P* plot results agreed with observations of the Weibull distribution. ANOVA was performed for experimental observations and modified model predictions. The test was conducted

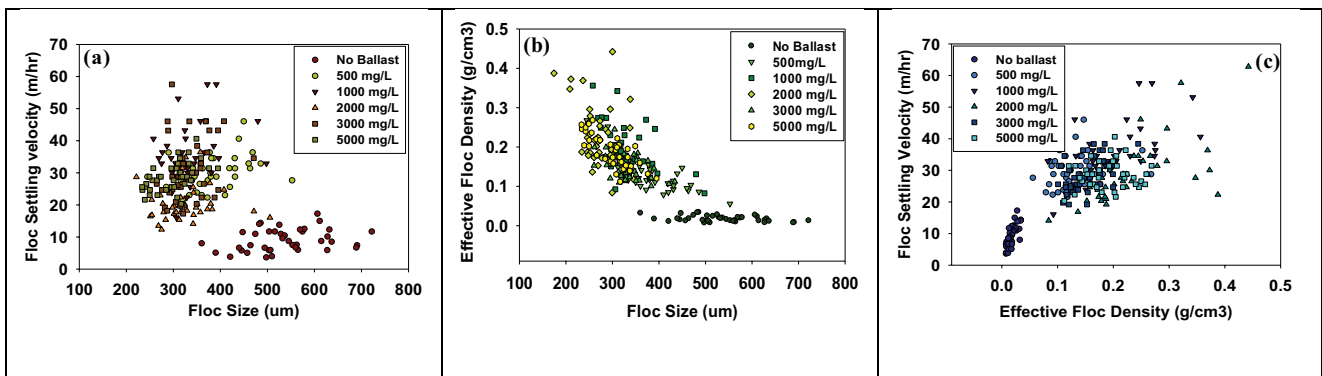


Fig. 3. Floc Size, effective density, and settling velocity relationship: (a) floc size vs settling velocity, (b) floc size vs effective floc density, and (c) effective floc density vs settling velocity.

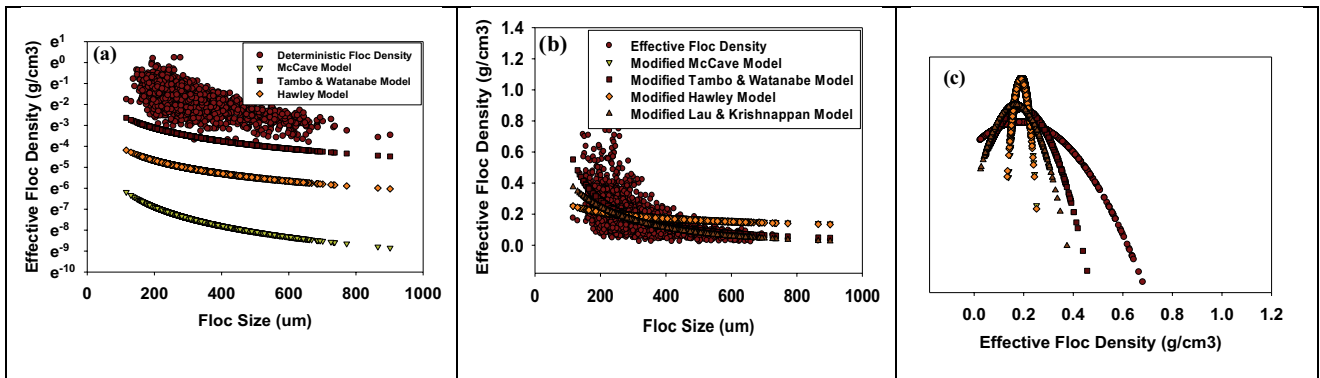


Fig. 4. Density model simulation with deterministic floc density: (a) existing models, (b) modified models, and (c) Weibull distribution curves for deterministic density and modified model predictions.

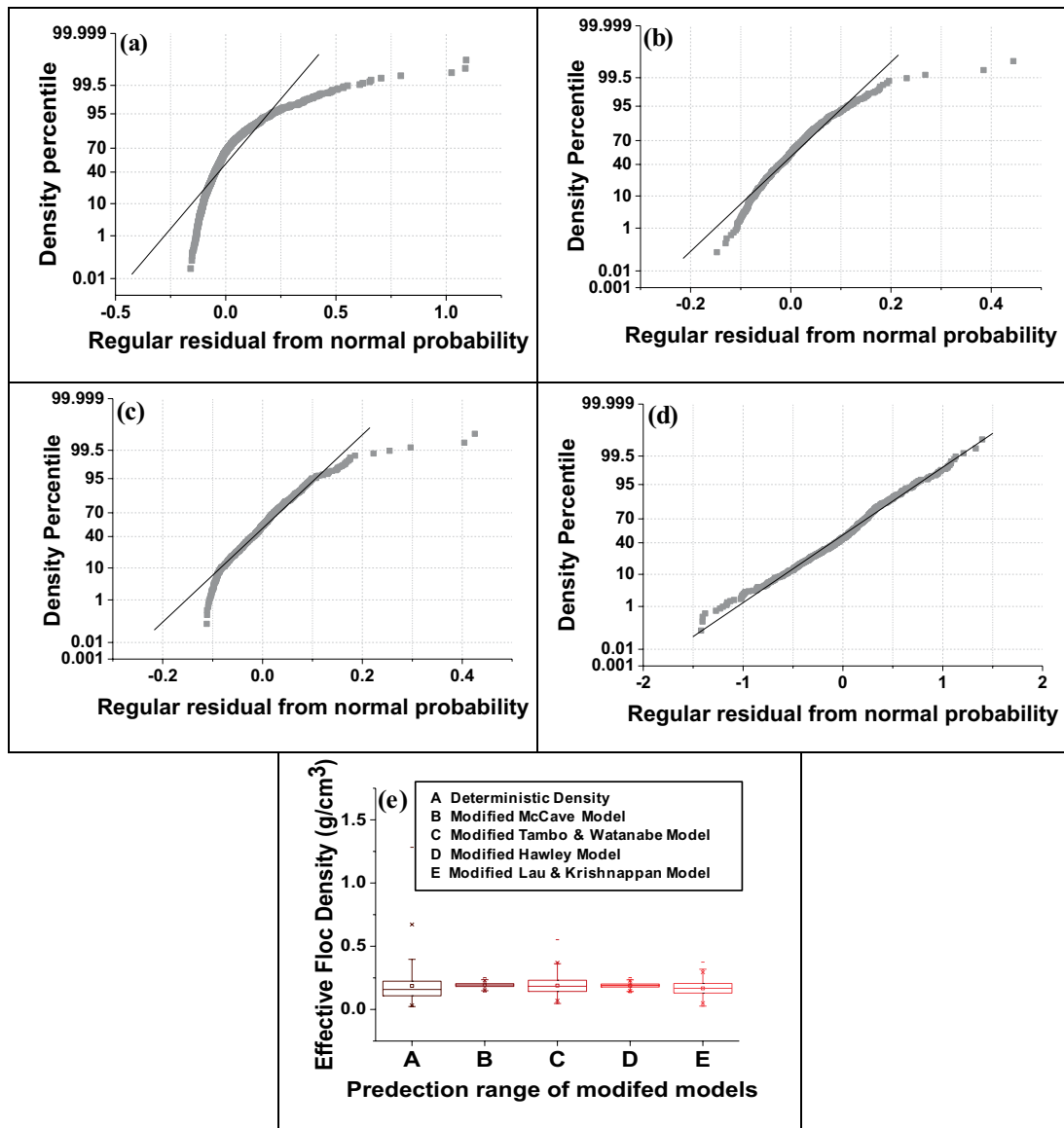


Fig. 5. Normal probability plots: (a) modified McCabe model, (b) modified Tambo and Watanabe model, (c) modified Hawley model, (d) modified Lau and Krishnappan model, and (e) ANOVA box chart of modified model density predictions compared with deterministic floc density.

under the null hypothesis that data means are equal at all levels. Determined and model-predicted density were input in OriginPro 2016 as raw data. Five levels were selected for data sets of predictions from four models and one data set of determined density values. Tukey’s test was performed in conjunction with ANOVA for comparing data means, and Levene’s test was incorporated for determining equality of variance. Box charts were drawn to compare predicted ranges with determined density values. The results revealed that the means were significantly different, nullifying the hypothesis. However, high R^2 for the modified models of Lau and Krishnappan and Tambo and Watanabe indicated that predictions of these models highly corresponded to experimental observations. Among all modified models under investigation, the modified model by Lau and Krishnappan with high R^2 value showed the highest matching of 87% between determined density values and model predictions with lower RMSE showing no significant variation among model and determined data sets; this also satisfies the significance level of the test with p -value < 0.05 , as shown in Table 2. The box chart comparison of data sets shown in Fig. 5(e) supports the conclusion from ANOVA results; the model prediction range for the model of Lau and Krishnappan was very close to the range of experimental observations.

The Pearson’s correlation test was conducted for determined floc density and model predictions using IBM SPSS Statistics 24 to check the correlation of model predictions with determined effective floc density. The test was conducted at 99% confidence level (at significance level 0.01), maintaining 1% margin of error. The results were completely in agreement with ANOVA and Weibull distribution results. As indicated in Table 3, all the model predictions significantly correlate with the determined floc density values. The significance (2 tailed) for models should be lower than test significance level of 0.01 to support the hypothesis

that the data correlation is not a result of any coincidence but the model-predicted values close to determined values. The significance for all models was under the benchmarked significance level (0.01), indicating strong correlation between model predictions and effective floc density. The higher Pearson’s correlation factor value of the modified model of Lau and Krishnappan (0.55) indicated that among all the model predictions, this model’s prediction was closer to the determined density values, which agrees with the results of P - P plots and ANOVA.

3.4. Evaluation of modified settling velocity models

The existing and modified velocity models were used to compute the settling velocity values as a function of floc size, and the computed values were then simulated with experimental settling velocity data sets obtained from the image analysis. The existing models were found to underestimate the velocity values of experimental observations, whereas the modified models were found to estimate the settling velocity values more closely, as shown in Figs. 6(a) and (b), respectively. The Weibull distribution was applied to model predictions and experimental observations. Comparing the generated curves, existing models did not show any correlation with the experimental velocity observations and observed settling velocity in a very narrow region of experimental velocity curve as shown in Fig. 6(c). Therefore, from these observations, it can be concluded that floc settling velocity cannot be determined as a function of floc size. However, floc size and density in combination can be used to predict floc settling velocity more accurately as floc density has been reported to be an important factor driving floc settling [5].

The floc size and settling velocity of ballasted flocs did not show any trend; thus, the empirical relationship between floc size and settling velocity could not be used to predict

Table 2
ANOVA for modified models’ comparison with determined density

Model	R^2 value	Coefficient of variation	Root mean square of error (RMSE)	F-value	P-value
Modified McCave model	0.66	0.61	0.11	1.45	1.3E-8
Modified Tambo & Watanabe model	0.84	0.31	0.06	1.44	4.9E-6
Modified Hawley model	0.77	0.07	0.01	1.94	5.6E-15
Modified Lau & Krishnappan model	0.87	0.27	0.04	1.77	9.7E-12

*The population means are significantly different (reported by OriginPro 2016).

Table 3
Pearson’s correlation test of model predictions with determined floc density

Model	Pearson correlation factor	Significance (2 tailed)
Modified McCave model	0.535	5.5E-137
Modified Tambo and Watanabe model	0.547	6.28E-144
Modified Hawley model	0.540	7.44E-140
Modified Lau and Krishnappan model	0.549	3.87E-145

*Correlation is significant at 0.01 level (2 tailed) (reported by SPSS program).

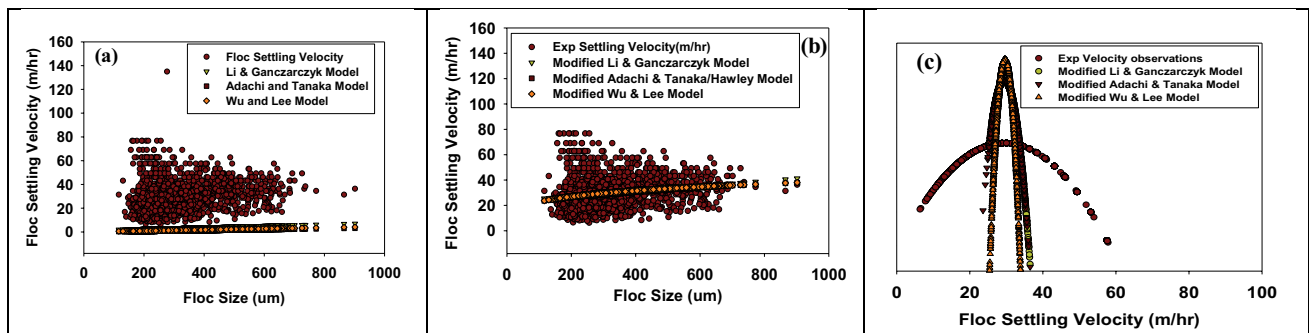


Fig. 6. Model velocity prediction simulation with experimental settling velocity; (a) existing models, (b) modified models, and (c) comparison of Weibull distribution curves of experimental velocity with modified models.

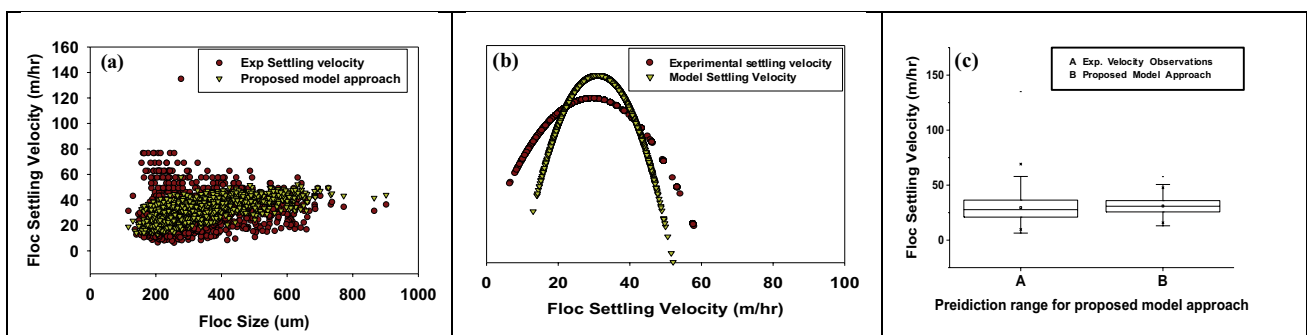


Fig. 7. Experimental velocity simulation with proposed model prediction; (a) predicted and experimental velocity plot, (b) Weibull distribution curves, and (c) ANOVA test box chart.

floc settling velocity. From this observation, it can be concluded that predicting floc settling velocity as a sole function of floc size for ballasted flocs is difficult because this type of flocs shows faster settling velocity trend attributed to the induced high-density ballast particles in addition to their compactness. Consequently, the modified velocity models that predict floc velocity as linear or power functions of floc size failed to predict the floc settling velocity for ballasted flocs. Therefore, the relationship of floc settling velocity with floc size and floc density in combination can provide more accurate predictions for ballasted flocs because floc size has a strong empirical relationship with effective floc density. Furthermore, effective floc density is directly proportional to floc settling velocity.

3.5. Proposed model approach

Most researchers developed floc settling velocity models based on Stokes' law which supports the calculation of floc settling velocity as a function of floc size, floc density, and drag coefficient [Eq. (1)]. Keeping the assumption of floc sphericity, Stokes' law was applied to the modified model of Lau and Krishnappan to determine settling velocity for ballasted flocs. The drag coefficient value was computed using the normal distribution peak value of Reynolds number (2.98). The determined floc settling velocity based on this approach was compared with experimental floc settling velocity. The results revealed that floc settling velocity can be accurately determined using Stokes' law with the modified model of Lau and Krishnappan, as clearly depicted

in Fig. 7(a). The Weibull distribution curve comparison revealed a strong correlation between predictions of this combined model and experimental velocity, as shown in Fig. 7(b).

The ANOVA results for the combined model and experimental values also showed considerably significant correlation among data sets, with a high R^2 value of 75%, satisfying the test significance level, and lower RMSE and coefficient of variation. The box charts representing the prediction range of the combined model and experimental values also closely matched, as shown in Fig. 7(c). The Pearson's correlation test also showed as significant correlation (successful significance (2 tailed) under the benchmarked test significance level) between model predictions using this approach and experimental values with high Pearson's coefficient value of 0.799, as shown in Table S5 in supplementary materials.

4. Conclusions

The applicability of existing models to estimate floc settling velocity was examined for ballasted flocs, and the results showed that the models underestimated the floc settling velocity because the associated parameters were not obtained from the flocs of BF. These models were modified based on experimental observations using image analysis for improving their prediction of ballasted flocs. A modified density model of Lau and Krishnappan was found to be the most appropriate for predicting the individual floc density. Model predictions were found to strongly agree with experimental results through ANOVA, and a satisfactory correlation

was found through Pearson's correlation tests. The modified velocity models could predict the velocity partially in agreement with experimental values, but they could not predict velocity variations. Experimental results revealed that settling velocity in BF can be predicted accurately by considering both floc density and floc size. Thus, Stokes' velocity model in combination with the modified density model of Lau and Krishnappan was proposed as best settling velocity model for BF. This modified velocity model showed significant agreement with experimental velocity observations. In ANOVA and Pearson's correlation test, this modified model provided predictions that matched with 75% of experimental observations, and thus, it can be effectively used for predicting settling velocity for ballasted flocs.

Symbols

V_f	—	Floc settling velocity
ρ_f	—	Floc density
ρ_w	—	Density of water at room temperature
$\rho_f - \rho_w$	—	Effective floc density
D_f	—	Floc diameter
ρ_s	—	Parent particle density (kaolin)
$\rho_s - \rho_w$	—	Effective parent particle density
d_s	—	Diameter of parent particles in suspension
Re	—	Reynolds number
C_d	—	Drag Coefficient
A_p	—	Projected area of floc
g	—	Gravitational force
μ	—	Viscosity of water

Acknowledgement

This study is supported by the Korea Ministry of Environment under the "Global Top Project (2016002110006)"

References

- [1] M. Zhang, F. Xiao, D. Wang, X. Xu, Q. Zhou, Comparison of novel magnetic polyaluminum chlorides involved coagulation with traditional magnetic seeding coagulation: coagulant characteristics, treating effects, magnetic sedimentation efficiency and floc properties, *Sep. Purif. Technol.*, 182 (2017) 118–127.
- [2] A. Ghanem, J. Young, F. Edwards, Settling velocity models applied to ballasted flocs: a review, *SABER. Revista Multidisciplinaria del Consejo de Investigación de la Universidad de Oriente*, 25 (2013) 247–253.
- [3] J. Nan, W. He, Characteristic analysis on morphological evolution of suspended particles in water during dynamic flocculation process, *Desal. Wat. Treat.*, 41 (2012) 35–44.
- [4] D.-H. Li, J.J. Ganczarzyk, Stroboscopic determination of settling velocity, size and porosity of activated sludge flocs, *Water Res.*, 21 (1987) 257–262.
- [5] A. Khelifa, P.S. Hill, Models for effective density and settling velocity of flocs, *J. Hydraul. Res.*, 44 (2006) 390–401.
- [6] N. Hawley, Settling velocity distribution of natural aggregates, *J. Geophys. Res.: Oceans*, 87 (1982) 9489–9498.
- [7] Y. Watanabe, Flocculation and me, *Water Res.*, 114 (2016) 88–103.
- [8] N. Tambo, Y. Watanabe, Physical characteristics of flocs—I. The floc density function and aluminium floc, *Water Res.*, 13 (1979) 409–419.
- [9] C.P. Johnson, X. Li, B.E. Logan, Settling velocities of fractal aggregates, *Environ. Sci. Technol.*, 30 (1996) 1911–1918.
- [10] J.C. Winterwerp, A simple model for turbulence induced flocculation of cohesive sediment, *J. Hydraul. Res.*, 36 (1998) 309–326.
- [11] B.G. Krishnappan, J. Marsalek, Modelling of flocculation and transport of cohesive sediment from an on-stream stormwater detention pond, *Water Res.*, 36 (2002) 3849–3859.
- [12] C. Kranenburg, The fractal structure of cohesive sediment aggregates, *Estuar. Coast. Shelf Sci.*, 39 (1994) 451–460.
- [13] I. McCave, Vertical flux of particles in the ocean, *Deep Sea Res. Oceanogr. Abstr.*, 22 (1975) 491–502.
- [14] Y.I. Lau, B.G. Krishnappan, Measurement of size distribution of settling flocs, NWRI Publication No. 97-223, National Water Research Institute, Environment Canada, Burlington, Ontario, Canada, 1997.
- [15] R. Wu, D. Lee, Hydrodynamic drag force exerted on a moving floc and its implication to free-settling tests, *Water Res.*, 32 (1998) 760–768.
- [16] D. Ghernaout, B. Ghernaout, Sweep flocculation as a second form of charge neutralisation—a review, *Desal. Wat. Treat.*, 44 (2012) 15–28.
- [17] Y. Adachi, Y. Tanaka, Settling velocity of an aluminium-kaolinite floc, *Water Res.*, 31 (1997) 449–454.
- [18] Y. Sun, C. Zhu, H. Zheng, W. Sun, Y. Xu, X. Xiao, Z. You, C. Liu, Characterization and coagulation behavior of polymeric aluminum ferric silicate for high-concentration oily wastewater treatment, *Chem. Eng. Res. Design*, 119 (2017) 23–32.
- [19] F. Ying, Investigation on flocculation process of composite poly-Si-Fe coagulant, *Desal. Wat. Treat.*, 30 (2011) 122–133.
- [20] W. Wei, X. Li, J. Zhu, M.-a. Du, Characteristics of flocs formed by polyaluminum chloride during flocculation after floc recycling and breakage, *Desal. Wat. Treat.*, 56 (2015) 1110–1120.
- [21] Y. Smaoui, M. Chaabouni, S. Sayadi, J. Bouzid, Coagulation–flocculation process for landfill leachate pretreatment and optimization with response surface methodology, *Desal. Wat. Treat.*, 57 (2016) 14488–14495.
- [22] Z. Wang, J. Nan, M. Yao, Y. Yang, Effect of additional polyaluminum chloride and polyacrylamide on the evolution of floc characteristics during floc breakage and re-growth process, *Sep. Purif. Technol.*, 173 (2017) 144–150.
- [23] M. Vlieghe, C. Frances, C. Coufort-Saudejaud, A. Liné, Morphological properties of flocs under turbulent break-up and restructuring processes, *AIChE J.*, 63.9 (2017) 3706–3716.
- [24] Y.M.S. Park, J.-O. Kim, Evaluation of the image analysis method using statistics for determining the floc size and settling velocity in ballasted flocculation, *Desal. Wat. Treat.*, 99 (2017) 102–106.
- [25] M. Lapointe, B. Barbeau, Characterization of ballasted flocs in water treatment using microscopy, *Water Res.*, 90 (2016) 119–127.
- [26] O.A. Mikkelsen, P.S. Hill, T.G. Milligan, Seasonal and spatial variation of floc size, settling velocity, and density on the inner Adriatic Shelf (Italy), *Cont. Shelf Res.*, 27 (2007) 417–430.
- [27] M. Aguilar, J. Saez, M. Llorens, A. Soler, J. Ortuno, Microscopic observation of particle reduction in slaughterhouse wastewater by coagulation–flocculation using ferric sulphate as coagulant and different coagulant aids, *Water Res.*, 37 (2003) 2233–2241.
- [28] D. Lee, G. Chen, Y. Liao, C. Hsieh, On the free-settling test for estimating activated sludge floc density, *Water Res.*, 30 (1996) 541–550.
- [29] J. Gregory, The role of floc density in solid-liquid separation, *Filtr. Separ.*, 35 (1998) 367366–367371.
- [30] G. Kemmer, S. Keller, Nonlinear least-squares data fitting in Excel spreadsheets, *Nat. Protoc.*, 5 (2010) 267–281

Supplementary Information

Table S1
Characteristics of ballast materials

Sr. No.	Ballast	(a)	(b)	(c)	(d)
(1)	Particle size (μm)	25	33	33	64
(2)	Zeta potential (mV)	-35.3	-37.8	+31.6	-44.3
(3)	Specific gravity	2.9	5.1	5.09	4.8
(4)	Formula	$\text{Fe}_3\text{O}_4/\text{SiO}_2$	$\text{Fe}_3\text{O}_4/\text{COOH}$	$\text{Fe}_3\text{O}_4/\text{NH}_2$	$\text{Fe}_3\text{O}_4/\text{SiO}_2$

Table S2
Jar test experimental conditions for formation of ballast-aided flocs

Parameters	Conditions
Raw water	Kaolin 200 mg/L (190 NTU, 170 SS mg/L)
pH	8
Temperature	20°C
Ballast dose (mg/L)	100–5,000 mg/L
Coagulant	PAC (10%), 30 mg/L
Rapid mixing	110 rpm (G-160/s), 3 min
Slow mixing	60 rpm (G-65/s), 15 min
Settling	15 min

Table S3
Input velocity and density model equations in origin program for computing values for variables

Sr. No.	Velocity model equations	Density model equations
(1)	$V_f = A + BD_f$	$\rho_f - \rho_w = \frac{a}{\left(\frac{D_f}{1}\right)^k}$
(2)	$V_f = AD_f^c$	$\rho_f - \rho_w = (\rho_s - \rho_w) \left(\frac{D_f}{d_s}\right)^a$
(3)	$V_f = AD_f^c *$	$\rho_f - \rho_w = D_f^c$
(4)	–	$\rho_f - \rho_w = (\rho_s - \rho_w) \exp(AD_f^c)$

*Eq. (3) is same as Eq. (2) but its regression is done using floc size in meters and settling velocity in meter per second.

Table S4
Drag coefficient as a function of flow condition (Gregory, Zabel, & Edzwald, 1999)

Reynolds number (Re)	Type of flow	Drag coefficient (C_d)
$10^{-4} \leq \text{Re} < 1$	Laminar	$C_d = \frac{24}{\text{Re}}$
$1 \leq \text{Re} < 1,000$	Transitional	$C_d = \frac{24}{\text{Re}} + \frac{3}{\text{Re}^{0.5}} + 0.34$
$1,000 \leq \text{Re} < 2 \times 10^5$	Turbulent	≈ 0.44
$> 2 \times 10^5$	Turbulent	≈ 0.1

Table S5
 Pearson’s correlation test of model predictions with effective floc density

Modified model	Pearson correlation factor	Significance (2 tailed)
Lau and Krishnappan model density-induced Stokes’ law model	0.799	1.58E-207

*Correlation is significant at the 0.01 level (2 tailed).

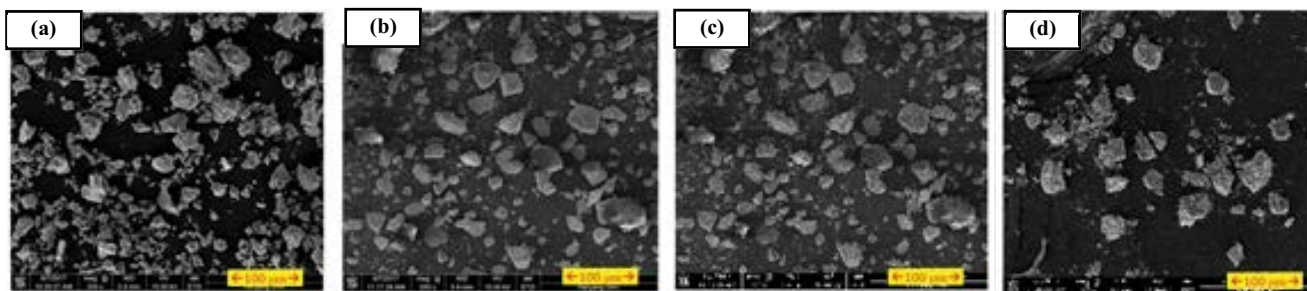


Fig. S1. SEM images; (a) 25 μm ballast, (b) 33 μm ballast negative surface charge, (c) 33 μm ballast positive surface charge, and (d) 64 μm ballast.



Fig. S2. Jar test apparatus.



Fig. S3. Vertical column image analyzer.



Fig. S4. CCD camera and light.

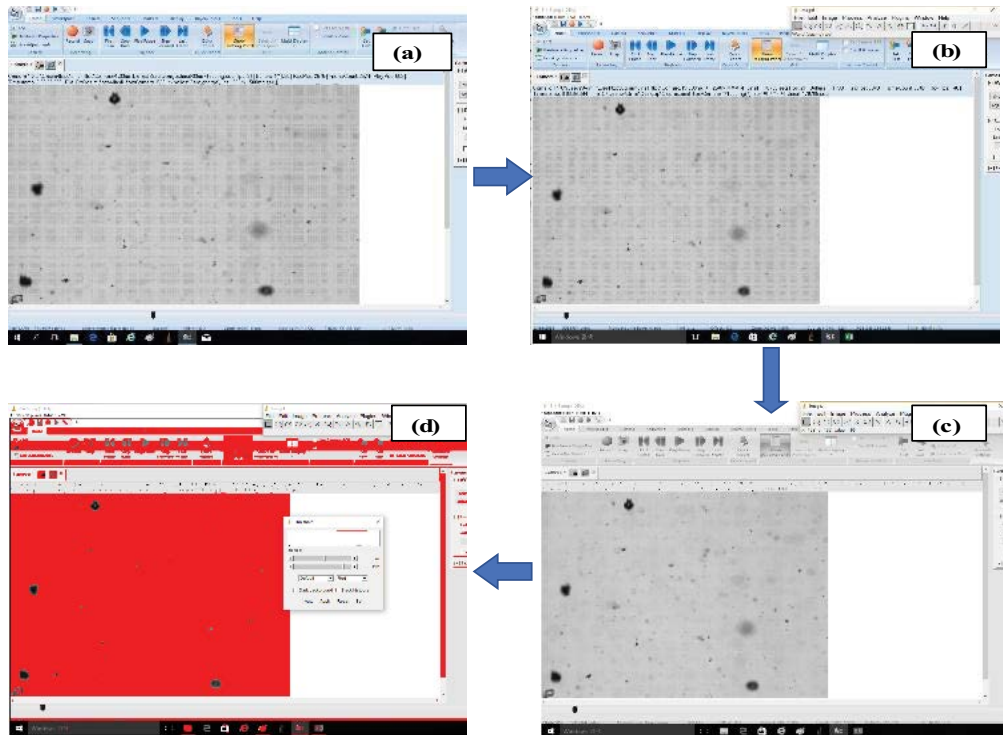


Fig. S5. Image analysis process: (a) recording floc settling using StreamPix, (b) floc frame transporting to image-J public domain software, (c) noise dis-pickle tool application to remove background blur flocs, and (d) threshold tool application to reveal floc boundaries.

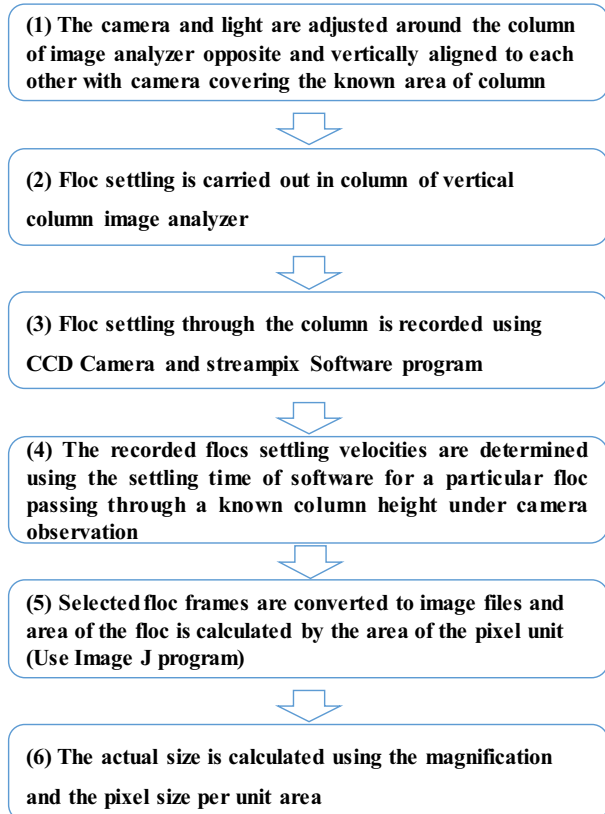


Fig. S6. Image analysis process flow chart.

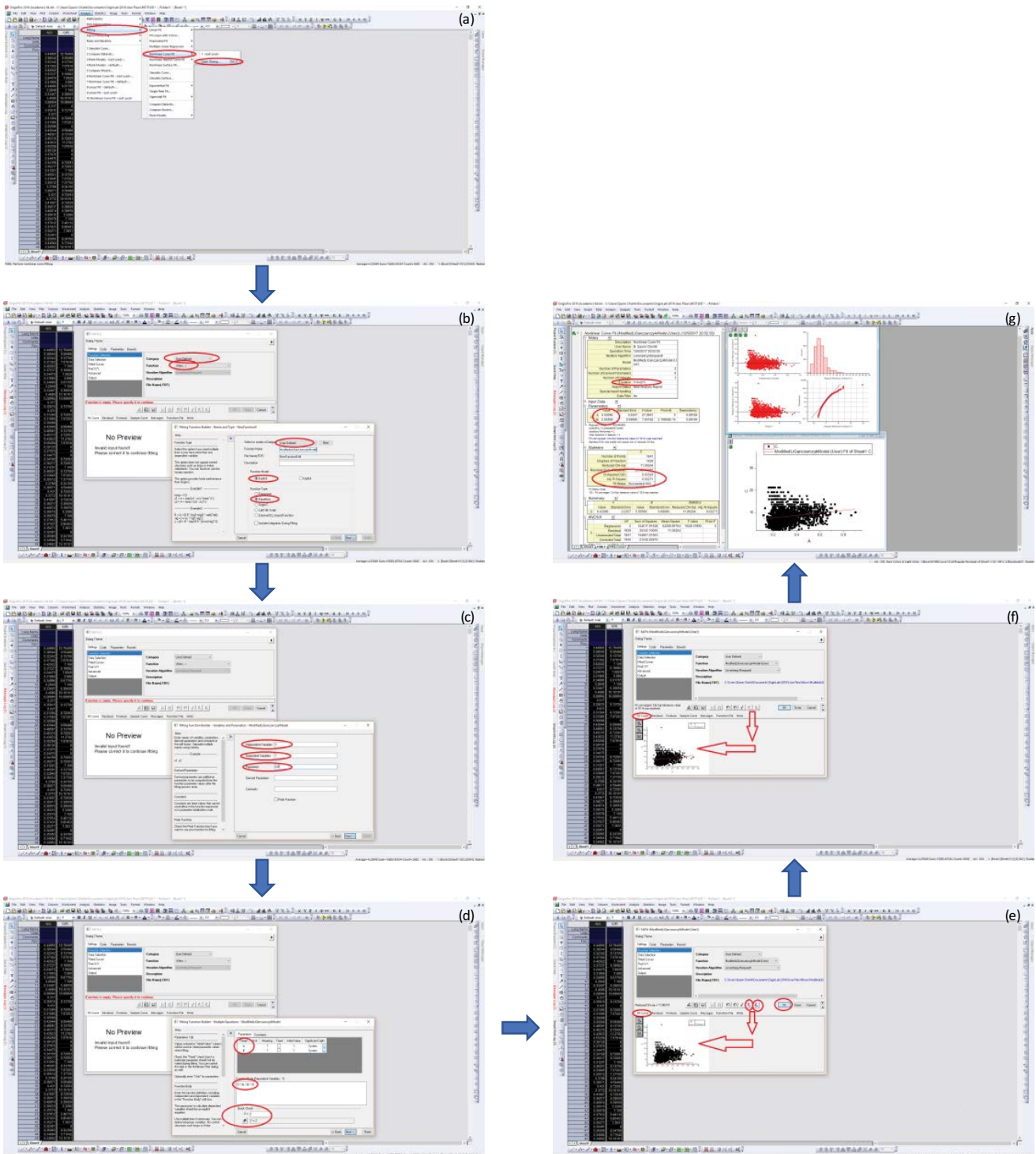


Fig. S7. Model modification process using origin software program: (a) selecting nonlinear curve fit in fitting tool of analysis wizard, (b) selecting user-defined model tab and equation tab, (c) defining independent and dependent variables and parameters (constants), (d) input model equation and testing workability of equation function by quick test tool, (e) previewing model curve and experimental/deterministic data, (f) simulating model curve by fitting tool with experimental/deterministic data, and (g) getting values for constant parameters at successful fit status and observing model line simulation with data and probability residual plots.